Asymmetric diffusion model for oblique-incidence reflectometry

Yaqin Chen (谌雅琴)[1*], Liji Cao (曹立基)[2], and Liqun Sun (孙利群)[1]

[1]*State Key Laboratory of Precision Measurement Technology and Instruments, Tsinghua University, Beijing 100084, China*

[2]*Division of Medical Physics in Radiology, German Cancer Research Center, Im Neuenheimer Feld 280, 69120 Heidelberg, Germany*

[*]*Corresponding author: yaqinchen@mail.tsinghua.edu.cn*

Received March 31, 2011; accepted May 9, 2011; posted on line July 11, 2011

A diffusion theory model induced by a line source distribution is presented for oblique-incidence reflectometry. By fitting to this asymmetric diffusion model, the absorption and reduced scattering coefficients μ_a and μ_s' of the turbid medium can both be determined with accuracy of 10% from the absolute profile of the diffuse reflectance in the incident plane at the negative position –1.5 transport mean free path (mfp′) away from the incident point; particularly, μ_s' can be estimated from the data at positive positions within 0–1.0 mfp′ with 10% accuracy. The method is verified by Monte Carlo simulations and experimentally tested on a phantom.

OCIS codes: 170.0170, 170.3660, 170.7050.

doi: 10.3788/COL201109.101701.

Knowledge about the optical properties, including the absorption coefficient (μ_a) and the reduced scattering coefficient ($\mu_s' = \mu_s(1–g)$), where μ_s is the scattering coefficient and g is the anisotropy factor of scattering, of biological tissues plays an important role for optical therapeutic and diagnostic techniques in medicine. Over the past two decades, many techniques have been developed to measure the optical properties of turbid media[1–3]. Oblique-incidence reflectometry is an attractive method for determining the optical properties of semi-infinite turbid media due to its simplicity and accuracy[4,5]. To deduce μ_a and μ_s' from a spatial distribution of diffuse reflectance produced by obliquely incident light, Lin *et al.*[5] proposed a diffusion theory model by using two isotropic scattering point sources–one positive source located at 1 transport mean free path (1 mfp′ $= 3D = (0.35\mu_a + \mu_s')^{-1}$, where D is the diffusion coefficient) measured along the optical path determined by Snell′s law below the surface and one negative image source above the surface. As a result, the positions of the point sources had a shift Δx in the x direction. By introducing this shift, the dipole-source model in Ref. [5] can accurately model the oblique-incidence diffuse reflectance falling outside the range of 1–2 mfp′ from the source. To determine μ_a and μ_s' using model in Ref. [5], the distance Δx should be measured by finding the apparent center of the symmetric reflectance profile at positions several mfp′ away from the source. Apparently, this is not good for the construction of a compact oblique-incidence reflectometer. In this letter, we introduce a different diffusion model induced by a line source distribution for oblique-incidence reflectometry.

Figure 1 shows a schematic illustration of the geometry concerned in this letter. An infinitely narrow light beam is incident upon a planar interface between a semi-infinite, highly scattering medium and a non-scattering medium with the refractive indices n_t and n_i. We set up a Cartesian coordinate system $Oxyz$ on the geometry. The origin O is the point of entry on the medium surface, the z axis is the normal of the surface pointing toward the inside of the medium, the x axis is along the projection of the pencil beam onto the planar surface ($z = 0$), and the y axis is perpendicular to both the x and z directions, pointing outward to form a right-handed Cartesian coordinate system. In such a coordinate system, the incident beam is located in the x-z plane, oriented at an angle α_i ($0 \leqslant \alpha_i < \pi/2$) with respect to the z axis, which is defined as the angle of incidence. When light enters the semi-infinite medium, ignoring the scattering interactions, it would be refracted to a transmission ray OL with an angle α_t to the z axis, as determined by Snell's law. However, light traveling in turbid media will suffer from multiple scattering events. Only the first scattering interactions of incident photons are situated along the unscattered-light transmission path OL. In diffusion approximation, scattering is assumed to be isotropic, thus each first scattering site can be treated as an isotropic point source. The strength of these sources will be determined by the optical properties of the medium and will exponentially decrease with the path length l_0 along the line OL measured from the incident point, similar to the exponentially decreasing line source distribution for normal-incidence beam in Ref. [6]. If assuming the light beam of unit intensity and taking account the Fresnel reflection at the boundary, the source term can be mathematically expressed as

$$S(x,y,z;l_0) = [1 - R_{\mathrm{Fres}}(\alpha_i, n_i, n_t)] \cdot$$

$$\mu_s' \int_0^{+\infty} \mathrm{e}^{-\mu_t' l_0} \delta(x - l_0 \sin\,\alpha_t)\delta(y)\delta(\mathrm{z} - l_0 \cos\,\alpha_t)\mathrm{d}l_0, \quad (1)$$

where δ is the Dirac delta function; R_{Fres} is the Fresnel reflection function[7]; $\mu_t' = 1/(3D)$ is the total reduced attenuation coefficient, where D has the same definition as in Ref. [5], $3D = (0.35\mu_a + \mu_s')^{-1}$.

Extrapolated boundary condition is used to account for the effect of Fresnel reflections due to the refractive

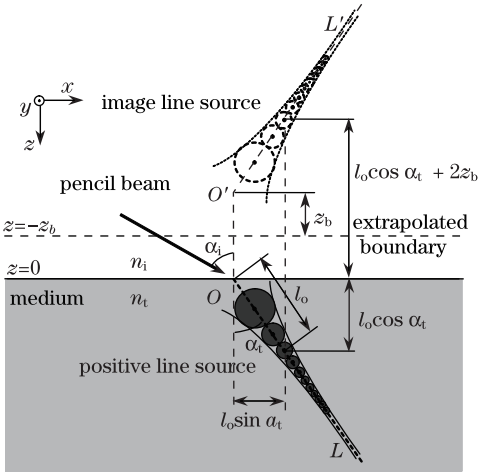

Fig. 1. Positions of the line sources in our diffusion theory model for oblique incidence.

index mismatch at the medium's surrounding boundary ($z = 0$)[7]. Under this boundary condition, the fluence rate is set to zero on an extrapolated boundary located at a distance z_b outside the turbid medium, that is,

$$\Phi(x, y, z = -z_b) = 0, \tag{2}$$

where $z_b = 2AD$; A is a coefficient related to the internal reflection, calculated by

$$A = \frac{1 + R_J}{1 - R_\Phi}, \tag{3}$$

in which

$$R_\Phi = \int_0^{\pi/2} 2R_{\rm Fres}(\theta, n_t, n_i)\sin\theta\cos\theta {\rm d}\theta, \tag{4}$$

$$R_J = \int_0^{\pi/2} 3R_{\rm Fres}(\theta, n_t, n_i)\sin\theta\cos^2\theta {\rm d}\theta. \tag{5}$$

To satisfy the extrapolated boundary condition, we also employed the method of images to derive the diffusion solutions by introducing a negative "image line source'', as depicted in Fig. 1. The image line source is along the line $O'L'$, which is the image of the line OL about the extrapolated boundary ($z = -z_b$). The strength of the image line source has the same distribution as the original photon line source, exponentially damped according to $\exp(-\mu_t' x/\sin\alpha_t)$ but the sign is negative. The resulting configuration of line source and its image can also be regarded as infinite pairs of dipole sources, located respectively at ($l_0\sin\alpha_t$, 0, $l_0\cos\alpha_t$) and at ($l_0\sin\alpha_t$, 0, $-2z_b - l_0\cos\alpha_t$) for any value of $l_0 \geqslant 0$. Each dipole source consists of an isotropic point source and its negative image source of equal strength. Consequently, solutions to the diffusion equation for an infinitely narrow beam with angle α_i incident on a homogeneous semi-infinite medium will be the infinite sum of solutions for every dipole source calculated in an infinite medium or can be calculated by integrating solutions for a dipole source at ($l_0\sin\alpha_t$, 0, $l_0\cos\alpha_t$) and at ($l_0\sin\alpha_t$, 0, $-2z_b - l_0\cos\alpha_t$) over $l_0 \geqslant 0$. In this study, the diffuse reflectance measured from the surface of the medium is our concerned physical quantity; the relationship between the fluence rate and the diffuse reflectance is defined as[7]

$$\begin{aligned} R(x,y) &= \int_0^{\pi/2} [1 - R_{\rm Fres}(\theta, n_t, n_i)] \frac{1}{2} [\Phi(x, y, z = 0) \\ &\quad + 3D\frac{\partial\Phi(x, y, z)}{\partial z}\Big|_{z=0} \cos\theta] \sin\theta\cos\theta {\rm d}\theta \\ &= \frac{1 - R_\Phi}{4}\Phi(x, y, z = 0) + \frac{1 - R_J}{2} D\frac{\partial\Phi(x, y, z)}{\partial z}\Big|_{z=0}. \end{aligned} \tag{6}$$

The final diffusion theory model of spatially diffuse reflectance distribution from the semi-infinite medium with oblique angle illumination is given by the following:

$$\begin{aligned} R(x,y)\Big|^{S(x,y,z;l_0)} &= \int_{-\infty}^{+\infty}\int_{-\infty}^{+\infty}\int_{-\infty}^{+\infty} S(x', y', z'; l_0) \\ &\quad \cdot R^{\rm G}(x,y)\Big|^{\delta(x-x')\delta(y-y')\delta(z-z')} {\rm d}x'{\rm d}y'{\rm d}z' \\ &= [1 - R_{\rm Fres}(\alpha_i, n_i, n_t)]\,\mu_s' \\ &\quad \int_0^{+\infty} R^{\rm G}(x,y)\Big|^{\delta(x-l_0\sin\alpha_t)\delta(y)\delta(z-l_0\cos\alpha_t)} {\rm e}^{-\mu_t' l_0} {\rm d}l_0, \end{aligned} \tag{7}$$

where $R^{\rm G}(x,y)\big|^{\delta(x-x_0)\delta(y-y_0)\delta(z-z_0)}$ is the diffuse reflectance solution with the extrapolated boundary condition for an isotropic point source located at (x_0, y_0, z_0) in the semi-infinite medium (i.e., $z_0 > 0$), which can be defined as

$$\begin{aligned} &R^{\rm G}(x,y)\Big|^{\delta(x-x_0)\delta(y-y_0)\delta(z-z_0)} \\ &= \frac{1 - R_\Phi}{4}\Phi^{\rm G}(x,y,z)\Big|_{z=0}^{\delta(x-x_0)\delta(y-y_0)\delta(z-z_0)} \\ &\quad + \frac{1 - R_J}{2} D\frac{\partial\Phi^{\rm G}(x,y,z)}{\partial z}\Big|_{z=0}^{\delta(x-x_0)\delta(y-y_0)\delta(z-z_0)}, \end{aligned} \tag{8}$$

in which

$$\begin{aligned} &\Phi^{\rm G}(x,y,z)\Big|_{z=0}^{\delta(x-x_0)\delta(y-y_0)\delta(z-z_0)} \\ &= \frac{1}{4\pi D}\left(\frac{{\rm e}^{-\mu_{\rm eff} r_{10}}}{r_{10}} - \frac{{\rm e}^{-\mu_{\rm eff} r_{20}}}{r_{20}}\right), \end{aligned} \tag{9}$$

$$\begin{aligned} &D\frac{\partial\Phi^{\rm G}(x,y,z)}{\partial z}\Big|_{z=0}^{\delta(x-x_0)\delta(y-y_0)\delta(z-z_0)} \\ &= \frac{1}{4\pi}\left[z_0\left(\mu_{\rm eff} + \frac{1}{r_{10}}\right)\frac{{\rm e}^{-\mu_{\rm eff} r_{10}}}{r_{10}^2}\right. \\ &\quad \left. + (z_0 + 2z_b)\left(\mu_{\rm eff} + \frac{1}{r_{20}}\right)\frac{{\rm e}^{-\mu_{\rm eff} r_{20}}}{r_{20}^2}\right], \end{aligned} \tag{10}$$

where $\Phi^{\rm G}(x,y,z)\big|^{\delta(x-x_0)\delta(y-y_0)\delta(z-z_0)}$ is the corresponding fluence rate solution for the point source at (x_0, y_0, z_0); $\mu_{\rm eff} = (\mu_a/D)^{1/2}$ is the effective attenuation coefficient; $r_{10} = [(x - x_0)^2 + (y - y_0)^2 + z_0^2]^{1/2}$; $r_{20} = [(x - x_0)^2 + (y - y_0)^2 + (z_0 + 2z_b)^2]^{1/2}$.

To test our diffusion model Eq. (7), we modified an open source Monte Carlo code[8] to accurately reproduce spatially resolved diffuse reflectance data under non-normal incident beam. In this letter, total simulated photons 10^8 were used for each simulation. We also presented the diffuse reflectance calculated by model in

Ref. [5] to compare the two diffusion models' performance. Numerical integration of Eq. (7) was used to obtain the diffuse reflectance for our diffusion model. However, the value at the entry point was excluded due to its convergence problem.

Figure 2 shows the two-dimensional distribution of diffuse reflectance generated by our diffusion model, Monte Carlo simulation, and model in Ref. [5] from a relatively low-absorbing high-scattering medium with optical properties $\mu_a = 0.01$ mm^{-1}, $\mu_s' = 1.0$ mm^{-1}, and relative refractive index $n_{rel} = n_t/n_i = 1.4$ illuminated by a beam with $\alpha_i = 60°$ (case I). In the Monte Carlo simulation, g equals 0.9. The spatial resolutions of x and y are the same at 0.1 mm, and the region of interest is limited to –10 mm $< x <$ 10 mm and –10 mm $< y <$ 10 mm. Looking at the images, we found that the outer portions were similar to each other. However, around the entry point, the distribution predicted by our model (Fig. 2(a)) presented a similarly non-circular symmetry as the resulting image generated by the Monte Carlo simulation (Fig. 2(b)); however, the image calculated by model in Ref. [5] (Fig. 2(c)) was circularly symmetric around the point shifting away from the point of entry. This was in accordance with our expectation since the two diffusion models (our model and that in Ref. [5]) respectively employed non-circularly and circularly symmetric source constructions.

Compared with that along the y axis, the diffuse reflectance profile along the x axis, i.e., in the incident plane, is more sensitive to the oblique incidence. Only the diffuse reflectance profile in the incident plane was considered in the later part. Figure 3(a) shows the diffuse reflectance profiles along the x axis of case I. Both diffusion models agreed with the Monte Carlo result at most positions. The model in Ref. [5] provided a somewhat better performance than our model, except at positive x positions very close to the entry point ($x = 0$). Instead, our diffusion model presented very good prediction-performance at positions extremely close to the incident point. To test the generality, we also conducted another simulation experiment for a relatively high-absorbing low-scattering medium with $\mu_a = 0.025$ mm^{-1}, $\mu_s' = 0.294$ mm^{-1}, and $n_{rel} = 1.33$ illuminated by a beam with $\alpha_i = 45°$ (case II). In this simulation, $g = 0.853$. The calculated diffuse reflectance profiles are illustrated in Fig. 3(b). The spatial resolutions of x and y and the range of x are of the same values with case I. These profiles looked like an enlarged view of the profiles in Fig. 3(a), although the optical properties and the incident angle were different for the two cases. The increased differences between the diffusion models and the Monte Carlo result appeared because the mfp′ in this case was 3.3 mm, much higher than the 1 mfp′ = 1.0 mm in case I. However, the prediction performance of our diffusion model was still good, particularly at positive x positions very close to the point of entry. Except at these positive x positions, the prediction performance of model in Ref. [5] was better than our model.

To quantitatively assess the model performance at different x positions, we calculated the root mean square error (RMSE) of the logarithm of the reflectance predicted by the diffusion models at different distance intervals in x. The results are listed in Table 1. From the listed RMSEs of both cases, we found that compared with model in Ref. [5] , our diffusion model achieved comparatively good performance at positions outside of the range from –1.5 to 3.0 mfp′, but much better performance over the range of 0–1 mfp′. By calculating the relative errors of the logarithm of the reflectance, we knew that our diffusion model had prediction accuracy of better than 6% at positions outside of the range from –0.8 to 0.2 mfp′ in x.

Based on the above analyses, we fitted the Monte Carlo data along the x axis at different intervals to our diffusion model with two fitted parameters μ_{eff} and D to determine the optical properties μ_a and μ_s'. Here, the reduced chi-square χ_v^2 was used as a measure of the goodness of fit between the data and the fitting model, and the Broyden–Fletcher–Goldfarb–Shanno (BFGS) quasi-Newton algorithm[9] was employed to minimize χ_v^2 in the optimization routine written in Python. The estimations of optical properties from the data of cases I and II at different x intervals are given in Table 2. We found that our diffusion model can be used to determine μ_a and μ_s', with accuracy better than 10% from only one side of the

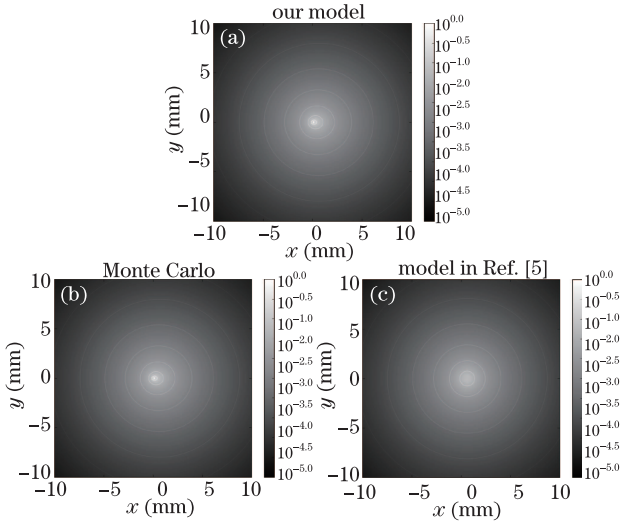

Fig. 2. Two-dimensional diffuse reflectance distributions from a semi-infinite turbid medium with optical properties $n_{rel} = 1.4$, $\mu_a = 0.01$ mm^{-1}, $\mu_s' = 1.0$ mm^{-1}, and $g = 0.9$ by an obliquely incident beam with $\alpha_i = 60°$, generated by (a) our diffusion theory model, (b) Monte Carlo simulation, and (c) model in Ref. [5].

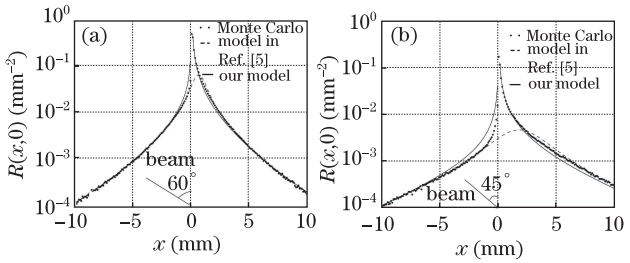

Fig. 3. Diffuse reflectance profiles along the x axis from a semi-infinite turbid medium (a) with optical properties $n_{rel} = 1.4$, $\mu_a = 0.01$ mm^{-1}, $\mu_s' = 1.0$ mm^{-1}, and $g = 0.9$ by an obliquely incident beam with $\alpha_i = 60°$ and (b) with optical properties $n_{rel} = 1.33$, $\mu_a = 0.025$mm^{-1}, $\mu_s' = 0.294$ mm^{-1}, and $g = 0.853$ illuminated by a beam with $\alpha_i = 45°$.

Table 1. RMSEs at Different Distance Intervals in x

Case	Diffusion Model	RMSEs at Different Intervals (mm) in x					
		(–10.0, –5.0)	(–5.0, –1.5)	(–1.5, 0)	(0, 1.0)	(1.0, 3.0)	(3.0, 10.0)
I	Ours	0.050	0.030	0.417	0.122	0.169	0.060
	Ref. [5]	0.061	0.025	0.103	0.944	0.110	0.038
II	Ours	0.071	0.253	0.732	0.048	0.099	0.183
	Ref. [5]	0.047	0.045	0.581	2.071	0.373	0.122

Table 2. Results of Estimation using our Diffusion Model

Data	Expected Values (mm^{-1})	Estimated Values (mm^{-1}) from the Data at Different x Positions (mm)				
		(–10.0, –5.0)	(–5.0, –1.5)	(0, 1.0)	(1.0, 3.0)	(6.0, 10.0)
Monte Carlo Case I	μ_a= 0.01	0.0106	0.0107	0.0	0.0026	0.0094
	$\mu_s' = 1.0$	0.973	0.971	1.049	1.329	1.073
Monte Carlo Case II	μ_a= 0.025	0.0251	0.0089	0.0	0.0056	0.0179
	$\mu_s' = 0.294$	0.266	0.180	0.258	0.276	0.390
Experiment	μ_a= 0.0061	–	0.0059	0.0	0.0042	–
	$\mu_s' = 1.004$	–	0.999	1.110	1.329	–

data at positions –1.5 or 6.0 mfp′ away from the incident point, and the reduced scattering coefficient μ_s' can even be derived from the data within the range of 0–1.0 mfp′, with estimation error of less than 10%. In comparison, the model in Ref. [5] is incapable of determining the optical properties under such conditions.

Aside from the above computer simulations, we constructed an oblique-incidence reflectometer based on a charge-coupled device (CCD) camera (ORCAII-BT, Hamamatsu Photonics K K, Japan) to test the applicability of our asymmetric diffusion model. A solid homogeneous phantom was obliquely illuminated by a collimated laser diode (670 nm LGTC series) at an angle of 53.2°. The phantom[10] was made of epoxy resin with scattering titanium dioxide particles and absorbing dye to provide $\mu_a = 0.01 \pm 0.002$ mm^{-1} and $\mu_s' = 1.0 \pm 0.02$ mm^{-1}at the wavelength of 800 nm. The refractive index of the resin n equals 1.56 ± 0.01. Figure 4(a) shows the experimental image of the diffusely reflected light I_R from the phantom. The spatial resolution was 0.04 mm in both the x and y directions, and the measured region was –5 mm $< x <$ 5 mm and –5 mm $< y <$ 5 mm. Since the oblique-incidence beam was not infinitely narrow but of a finite size, the center part of the image around the entry point broadened to a certain extent.

With the assumption of $n_{rel} = 1.56$, we first used model in Ref. [5] to fit the experimental data along the x axis to obtain the phantom's optical properties μ_a and μ_s' at the wavelength of 670 nm as well as the intensity of the laser beam. Before fitting, we searched for the center of the diffuse reflection profile at positions far away from the light entry point by satisfying the symmetry relation $I_R(x, 0) = I_R(-x+2\Delta x, 0)$. The shift Δx, D, and 1 mfp′ were measured to be 0.51, 0.33, and 0.99 mm, respectively. Then by fitting the data at positions ±1.5 mfp′ away from the source to Lin *et al.*'s diffusion model (Δx = 0.51 mm) with two fitted parameters – μ_{eff} and an intensity proportionality factor α – the phantom's optical properties at 670 nm were determined to be μ_a = 0.0061 mm^{-1} and μ_s' = 1.004 mm^{-1}; the intensity of the laser beam was represented by α = 29 407.35; the corresponding χ_v^2 was 0.0022. Compared with the phantom's optical properties at 800 nm (μ_a = 0.01±0.002 mm^{-1} and μ_s' = 1.0 ± 0.02 mm^{-1}), only the absorption coefficient changed clearly with the wavelength.

By using the intensity factor α obtained by model in Ref. [5] , we fitted the logarithm of the absolute diffuse reflection along the x axis at different positions to our diffusion model with fitted parameters of μ_{eff} and D. The relative refractive index n_{rel} was also assumed to be 1.56. The estimations of the phantom's optical properties are listed in Table 2. From the experimental data at (–5.0, –1.5) mm, we could very accurately estimate the optical properties to be $(\mu_a)_e$ = 0.0059 mm^{-1} and $(\mu_s')_e$ = 0.999 mm^{-1}, and the corresponding χ_v^2 was 0.0027. However, due to the effect of the used laser beam size, μ_s' could be determined to be 1.110 mm^{-1}, with accuracy that is somewhat lower than 10% from the data within (0, 1.0) mm and with a larger χ_v^2 = 0.303.

Figure 4(b) shows the profiles of the diffuse reflection along the x axis obtained by the experiment and predicted by model in Ref. [5] using μ_a = 0.0061 mm^{-1} and μ_s' = 1.004 mm^{-1} and by our proposed model using $(\mu_a)_e$ = 0.0059 mm^{-1} and $(\mu_s')_e$ = 0.999 mm^{-1} (n_{rel} = 1.56). The results by model in Ref. [5] agreed very well with the experiment at most positions except for –1.0 mm $< x <$ 2.0 mm (χ_v^2 = 0.0022), whereas the profile calculated by our diffusion model was also in very good agreement with the measurement data in the fitted interval of –5.0 mm $< x <$ –1.5 mm (χ_v^2 = 0.0027).

In conclusion, we develope an asymmetric diffusion theory model for oblique-incidence reflectometry. The model is originated by replacing the original oblique-incidence beam with an exponentially decreasing line

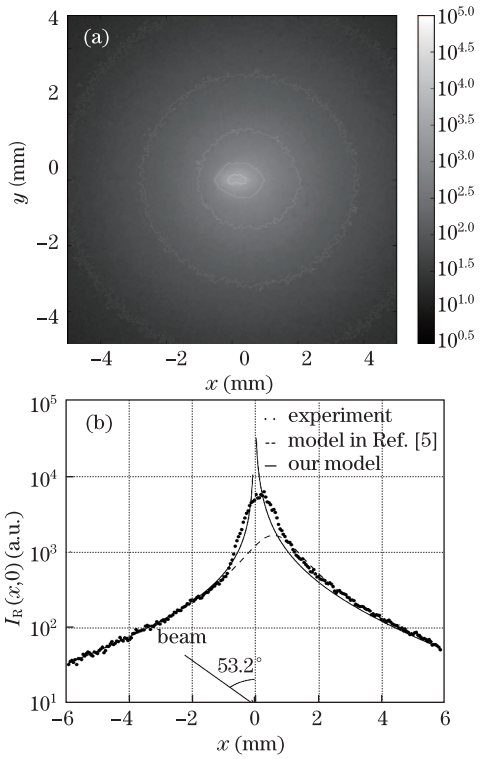

Fig. 4. (a) Diffuse reflection image from a phantom with a laser beam incident at $\alpha_i = 53.2°$ measured by an oblique-incidence video reflectometer; (b) diffuse reflection profiles along the x axis obtained by the experiment and predicted by model in Ref. [5] with $\mu_a = 0.0061$ mm^{-1} and $\mu_s' = 1.004$ mm^{-1} and by our proposed diffusion model with $(\mu_a)_e = 0.0059$ mm^{-1}, $(\mu_s')_e = 0.999$ mm^{-1}, $n_{rel} = 1.56$, and $\alpha = 2$ 9407.35.

source inside the medium and is derived through the combination of the extrapolation boundary condition and the method of images. Based on the Monte Carlo study, our diffusion model is able to predict the asymmetric distribution of diffuse reflectance in the incident plane due to non-normal incidence with accuracy better than 6% at positions in the range from –0.8 to 0.2 mfp′ away from the entry point ($x = 0$). Compared with model in Ref. [5], our diffusion model presents a much better prediction performance at positive x positions in the range of 0–1 mfp′, which are extremely close to the incident point, and achieves comparatively good performance at x positions outside of the range from –1.5 to 3.0 mfp′. After calibrating the intensity of the light source, our diffusion model can be used to determine the optical properties μ_a and μ_s' with accuracy better than 10% from only one side of the data along the x axis at positions –1.5 or 6.0 mfp′ away from the incident point. Specifically, μ_s' can be derived from the data within the range of 0–1.0 mfp′ in x, with estimation error of less than 10%. The accuracy of our asymmetric diffusion model has also been testified by an oblique-incidence video reflectometer measured on a phantom with the optical properties determined in Ref. [5]. By using our diffusion model to fit the absolute profile of diffuse reflection at negative x positions –1.5 mfp′ away from the incident point, we can very accurately estimate the phantom's optical properties μ_a and μ_s'. Since the used laser beam is of a finite size, the experimental data within the range of 0–1.0 mfp′ in x cannot be accurately described by our diffusion model, which is valid for an infinitely narrow beam. Nevertheless, we can still obtain μ_s' with a relatively lower accuracy from the data at 0–1.0 mfp′ by fitting it to our model. Our diffusion model will clearly be very useful for the development of a compact reflectometer probe in the applications of oblique-incidence reflectometry.

The authors thank Prof. Jeremy C. Hebden of University College London for loaning the homogeneous phantom used in this study to test our diffusion theory model.

References

1. A. J. Welch and M. J. C. van Gemert, *Optical-Thermal Response of Laser-Irradiated Tissue* (Springer, New York, 2011).
2. C. Li, H. Zhao, Q. Wang, and K. Xu, Chin. Opt. Lett. **8,** 173 (2010).
3. Y. Ma, F. Gao, P. Ruan, F. Yang, and H. Zhao, Chin. Opt. Lett. **8,** 206 (2010).
4. L. Wang and S. L. Jacques, Appl. Opt. **34,** 2362 (1995).
5. S. Lin, L. Wang, S. L. Jacques, and F. K. Tittel, Appl. Opt. **36,** 136 (1997).
6. T. J. Farrell, M. S. Patterson, and B. Wilson, Med. Phys. **19,** 879 (1992).
7. R. C. Haskell, L. O. Svaasand, T. Tsay, T. Feng, M. S. McAdams, and B. J. Tromberg, J. Opt. Soc. Am. A **11,** 2727 (1994).
8. L. Wang, S. L. Jacques, and L. Zheng, Comput. Meth. Programs Biomed. **47,** 131 (1995).
9. D. F. Shanno and K. H. Phua, ACM Trans. Math. Software **2,** 87 (1976).
10. M. Firbank and D. T. Delpy, Phys. Med. Biol. **38,** 847 (1993).